Received: 17 April 2019 | Accepted: 6 May 2019

DOI: 10.1002/pamm.201900058

Particle accumulation in high-Prandtl-number liquid bridges

Ilya Barmak[1,*], **Francesco Romanò**[1,2,**], and **Hendrik C. Kuhlmann**[1,***]

[1] Institute of Fluid Mechanics and Heat Transfer, TU Wien, 1060 Vienna, Austria

[2] Department of Biomedical Engineering, University of Michigan, Ann Arbor, Michigan 48109-2099, USA

Particle accumulation in high-Prandtl-number (Pr $= 68$) thermocapillary liquid bridges is studied numerically. Randomly distributed small rigid non-interacting spherical particles are found to cluster in particle accumulation structures. The accumulation is found to be caused by a finite-particle-size effect when the particles move close to the impermeable flow boundaries. The extra drag force experienced by a particle near the boundaries creates a dissipation in the dynamical system describing the particle motion. This causes particles to be attracted to regions in or near Kolmogorov-Arnold-Moser tori of the unperturbed flow field.

1 Introduction

Small spherical particles have been found to cluster in particle accumulation structures (PAS) in liquid bridges with Pr $= 4$ [1] and Pr $= 28$ [2]. This type of PAS is called *finite-size coherent structures* (FSCS) [2] and was shown to be generic for incompressible flows in which the repulsive particle–boundary interaction (PBI) forces are dominating forces on a particle acting in the bulk [3]. The thermocapillary flow under consideration (5 cSt silicone oil, Pr $= 68$) is characterized by much thinner thermal boundary layers than in moderate-Prandtl-number liquid bridges simulated previously. Therefore, the numerical resolution requirements are tighter, in particular, near the moving thermocapillary free surface. For a qualitative prediction of PAS the inelastic collision model [1] of the PBI has proven successful. For an accurate modeling, however, the only parameter Δ of the collision model, depending on particle size, density and flow parameters, should be determined carefully [2]. To avoid estimating Δ, we employ a more physically-based PBI model which makes use of the lubrication-induced drag acting on the particle in direction normal to the boundary [4].

2 Problem Formulation

A cylindrical liquid bridge of length d and radius R made by an incompressible fluid with Pr $= 68$ is considered under zero-gravity conditions between two coaxial rods with temperatures $T_{\text{cold}} = T_0$ and $T_{\text{hot}} = T_0 + \Delta T$ (Fig. 1a), neglecting flow-induced surface deformations. The fluid motion is driven by thermocapillary stresses caused by the spatial variation of the surface tension $\sigma(T(\vec{x},t))$. The governing equations [1] are solved subject to no-slip/no-penetration/constant-temperature boundary conditions on the rods and imposing thermocapillary stresses and adiabatic conditions on the free surface (neglecting viscous stresses and heat fluxes in the ambience). The fluid motion is then determined by the thermocapillary Reynolds number $\text{Re} = \gamma \Delta T d/\rho_f \nu^2$ (γ: surface tension coefficient, ρ_f: density, ν: kinematic viscosity), the aspect ratio $\Gamma = d/R$ of the liquid bridge, and Pr. For the high Reynolds numbers considered ($\text{Re} > \text{Re}_c \approx 300$ [5]), the flow $\vec{u}(\vec{x},t)$ arises as a three-dimensional hydrothermal wave (HTW) traveling azimuthally.

The motion of a small spherical particle is modeled by the simplified Maxey-Riley (SMR) equation [6] in the frame of reference rotating with the same angular velocity $\vec{\Omega} = \Omega \vec{e}_z$ as the HTW. The particle motion is determined by the steady flow $\vec{U}(\vec{x}) = \vec{u}(\vec{x},t) - \Omega \vec{e}_\varphi$ in the rotating frame, the initial conditions, the particle-to-fluid density ratio $\varrho = \rho_p/\rho_f$, and the Stokes number $\text{St} = 2\varrho a^2/9$, where $a = a_p/d$ is the dimensionless radius of the particle.

The SMR equation breaks down near the boundaries, because PBI forces due to the finite particle size are not included in the SMR equation. Therefore, we impose additional wall-normal drag forces in a uniform boundary layer of thickness $\Delta_B = 3a$ (cutoff distance) on all boundaries according to the solutions of Brenner [8] for a plane wall and a free surface.

3 Results and Discussion

The flow for Pr $= 68$ is obtained numerically using OpenFOAM on a block-structured mesh made of ≈ 21.5 million grid points. For $\Gamma = 1$ and $\text{Re} = 1500$ the HTW has a fundamental wave number $m = 1$ and an angular velocity $\Omega = 12.29$ (in the units of ν/d^2). The high grid resolution enables identifying various sets of Kolmogorov–Arnold–Moser (KAM) tori in the flow $\vec{U}(\vec{x})$.

* Corresponding author: e-mail ilya.barmak@tuwien.ac.at, phone +43 1 58801 32232

** e-mail francesco.romano@tuwien.ac.at

*** e-mail hendrik.kuhlmann@tuwien.ac.at

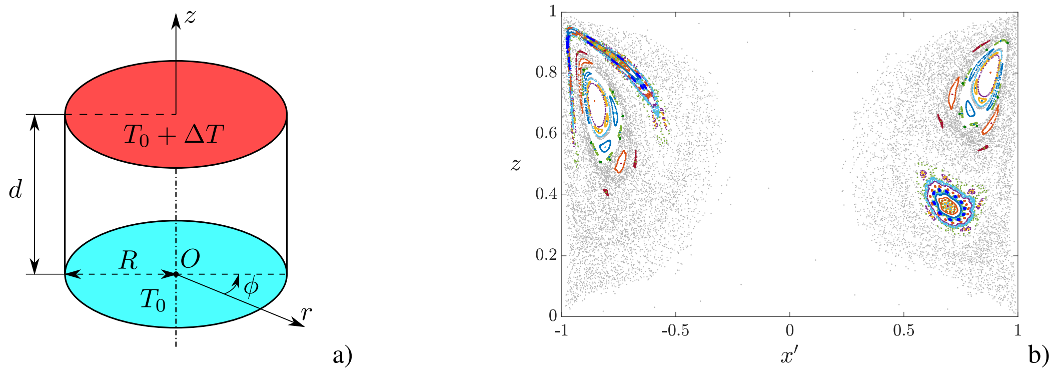

Fig. 1: a) Sketch of a cylindrical liquid bridge. b) Poincaré section in the (x', z)-plane ($\varphi = \varphi_{\text{max}} + \pi/4$, [7]) for Pr $= 68$, $\Gamma = 1$, Re $= 1500$, and Bi $= 0$. Poincaré points of chaotic (regular) streamlines are indicated in gray (color).

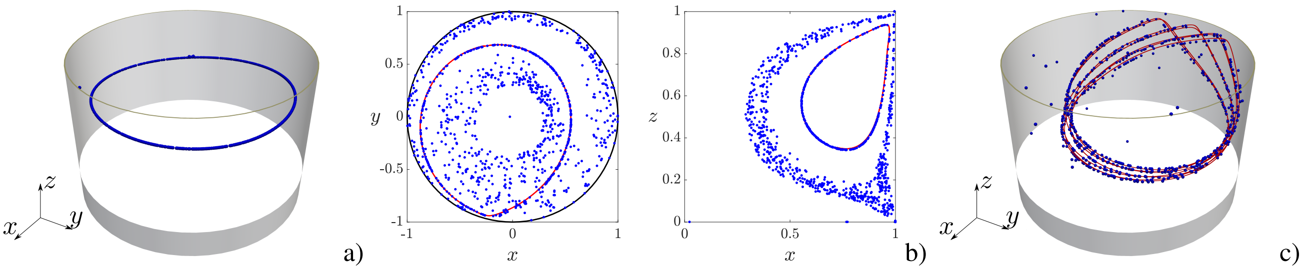

Fig. 2: PAS at $t = 340$ for $\Gamma = 1$ and 1000 density-matched particles ($\varrho = 1$). (a) Re $= 1500$ and $a = 0.02$. (b) Closed streamline (red) and axial and azimuthal projections of PAS (blue) for Re $= 1500$ and $a = 0.004$. (c) Closed streamline (red) and PAS (blue) for Re $= 2250$ and $a = 0.004$ using the collision model [1] with $\Delta = 2a$.

The topology of the regular streamlines is quite intricate [7]. Figure 1b shows a Poincaré section on the plane $\varphi = \varphi_{\text{max}} + \pi/4$, where φ_{max} maximizes $T(r = 1, \varphi, z = 0.5)$. Two major regular regions with KAM tori exist, one of which is extremely squeezed near the free surface and towards the hot corner. The flow topology has a strong influence on PAS for density-matched particles: after $t = 340$ (units of d^2/ν) thousand particles with $a = 0.02$ and $\varrho = 1$, initially randomly distributed and velocity matched, cluster on a periodic orbit near a closed streamline (Fig. 2a). Smaller particles ($a = 0.004$, $\varrho = 1$), however, cluster on another periodic orbit and on a separated diffuse structure (Fig. 2b), while the major part of the volume has become depleted of particles. The sharp attractor corresponds to a closed streamline, while the diffuse structure forms in the chaotic sea. The minimum distances between the periodic attractor and the top wall and the free surface are distinctively larger than the cutoff distance Δ_B. Therefore, the periodic orbit cannot have been created solely by the boundary effect. Another effect, currently under investigation, which might contribute to the sharp clustering of density-matched particles is based on amplification of a minute velocity mismatch by the very high strain of the flow field near the hot corner [6]. Heavy particles of the same size ($\varrho > 1$) do not cluster near the closed streamline. Rather, they approach the hot corner very closely and settle on the diffuse attractor in the chaotic sea. These results, obtained using Brenner's drag formulae, can also be reproduced using the simpler inelastic collision model with $\Delta = a$. However, the particle dynamics near the boundaries and, as a consequence, the time evolution of PAS are different.

As the Reynolds number is increased, the KAM structures become even more slender near the free surface. An example for a periodic PAS at Re $= 2250$ is shown in Fig. 2c. The attracting orbit is near a closed streamline which makes seven revolutions about the axis.

Acknowledgements This work has been supported by ESA through contract no. 4000121111/17/NL/PG/pt.

References

[1] E. Hofmann and H. C. Kuhlmann, Phys. Fluids **23**, 072106 (2011).
[2] F. Romanò and H. C. Kuhlmann, Phys. Rev. Fluids **3**, 094302 (2018).
[3] F. Romanò, H. Wu, and H. C. Kuhlmann, Int. J. Multiphase Flow **111**, 42–52 (2019).
[4] F. Romanò, P. Kunchi Kannan, and H. C. Kuhlmann, Phys. Rev. Fluids **3**, 094302 (2019).
[5] V. Shevtsova, A. Mialdun, H. Kawamura, I. Ueno, K. Nishino, and M. Lappa, Fluid Dyn. Mater. Process. **7**, 1–27 (2011).
[6] A. Babiano, J. H. E. Cartwright, O. Piro, and A. Provenzale, Phys. Rev. Lett. **84**, 5764–5767 (2000).
[7] H. C. Kuhlmann and F. Romanò, Midterm report: Modelling support to ESA-JAXA JEREMI project on ISS., Tech. rep., ESA, 2018.
[8] H. Brenner, Chem. Eng. Sci. **16**, 242–251 (1961).

